Introduction to PET Instrumentation

Timothy G. Turkington

Department of Radiology, Duke University Medical Center, Durham, North Carolina

Objective: The purpose of this paper is to introduce technologists to the basic principles of PET imaging and to the instrumentation used to acquire PET data. PET imaging is currently being done on a variety of imaging system types, and the technologist will be introduced to these systems and learn about the basic physical image-degrading factors in PET. After reading this article, the technologist should be able to describe the basics of coincidence imaging, identify at least 3 physical degrading factors in PET, and describe 2 different types of PET scanning systems.

Key Words: PET; positrons; instrumentation

J Nucl Med Technol 2001; 29:1–8

POSITRON PHYSICS

PET imaging relies on the nature of the positron and positron decay. The positron was first conceived by P.A.M. Dirac in the late 1920s, in his theory combining quantum mechanics and special relativity. It was experimentally discovered in 1932, the same year as the neutron. The positron is the antimatter counterpart to the electron, and therefore has the same mass as the electron but the opposite charge.

Positron Decay

When a nucleus undergoes positron decay, the result is a new nuclide with 1 fewer proton and 1 more neutron, as well as the emission of a positron and a neutrino:

$$^A_Z X_N \rightarrow\ ^A_{Z-1} Y_{N+1}\ +\ e^+\ +\ v. \qquad (1)$$
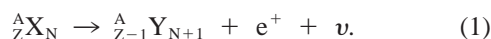
The radionuclides that decay via positron emission are proton-rich and move closer to the line of stability while giving off a positive charge. The neutrino is very light, if it has any mass at all, and interacts only very weakly with other particles. It is therefore not directly relevant to nuclear medicine. However, its presence in the positron decay makes the energy of the positron variable, as opposed to gamma emissions, which are of a fixed energy for a given radionuclide.

The most commonly used PET radionuclides are shown in Table 1. One characteristic is a short half-life. These radionu-

clides, which are cyclotron-produced, are also small atoms and are more likely to be found in biochemically relevant molecules than technetium or indium atoms, for example.

Positron Annihilation

As positrons pass through matter, they experience the same interactions as electrons, including loss of energy through ionization and excitation of nearby atoms and molecules. After losing enough energy, and having traveled a distance in the neighborhood of 1 mm (depending on the initial positron energy), the positron will annihilate with a nearby electron:

$$e^+\ +\ e^-\ \rightarrow\ \gamma\ +\ \gamma. \qquad (2)$$
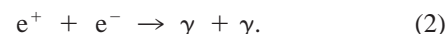
The energy of a particle has 2 components: its energy of motion and its mass. In the annihilation process described above, the initial energy is from the electron and positron masses, since they are moving relatively slowly at the time of the interaction, and the final energy is the combined energies of the photons, which have no mass. Conservation of energy and momentum dictate, therefore, that the 2 photons are emitted each with an energy of 511 keV (the electron mass times the speed of light squared) and in opposite directions, as shown in Figure 1.

COINCIDENCE DETECTION

The simultaneous emission of the 2 photons in opposite directions is the basis of coincidence detection and coincidence imaging.

A Coincidence Event

Imagine a ring of radiation detectors as shown in Figure 2. Within the ring is a patient in whom a positron emission has occurred. The positron moves a short distance in a random direction, slowing down until it annihilates with an electron, yielding two 511-keV photons, which are also emitted in a random direction. Although most of the annihilation photons will not be detected, some will remain in the plane of the detector ring, and 2 of the detectors will be hit, yielding

TABLE 1
Some Commonly Used PET Radionuclides

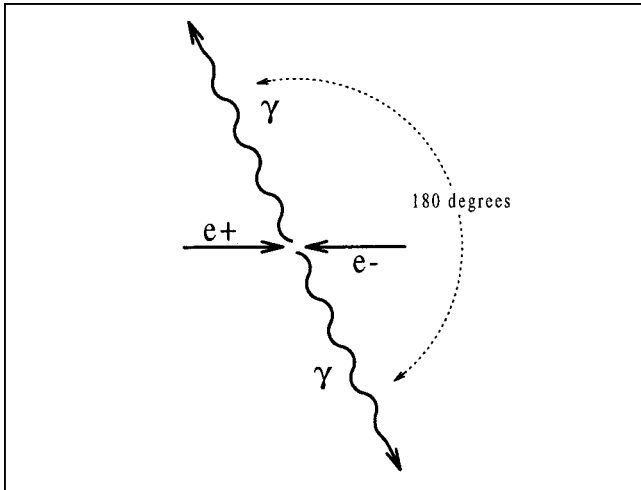| Nuclide	Halflife
^{11}C	20.3 min
^{13}N	9.97 min
^{15}O	124 sec
^{18}F	110 min

FIGURE 1. Diagram of electron–positron annihilation, producing 2 511 keV photons leaving in opposite directions.

FIGURE 2. Coincidence event detected in ring PET scanner.

electronic signals. The simultaneous pulses from the detectors indicate that an annihilation occurred somewhere along the path between the detectors. This is because the photons leave the annihilation point in opposite directions. The path between 2 detectors is referred to as a line of response (LOR). The simultaneous detection of 2 photons is referred to as a "coincidence". This meaning is very different from the common usage of the term "coincidence" to mean that 2 events happened without common cause. The number of coincidence events occurring between detectors indicates how much radioactivity there was on the LOR between the detectors.

Projections

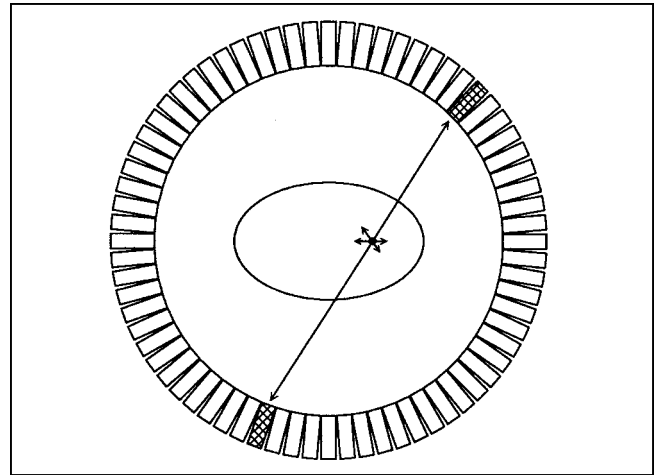Each pair of detectors in the ring defines a possible emission path. Over the course of a PET scan, the system is counting how many times each pair of detectors is hit in coincidence. For a ring with n detectors, there are $n^2/2$ ways to pair up the detectors, so a great deal of information is recorded.

One way to represent the raw data is to group together parallel LORs. For example, in Figure 3, the vertical LORs are depicted by solid lines. This set of LORs is a projection view of the radioactivity distribution in the body in that slice, similar to what would be obtained from a collimated gamma camera situated either at the top or the bottom of the patient. The other angles are formed similarly, and one of them is depicted with dashed lines in Figure 3.

The composite grouping of all angles is called a sinogram. In the sinogram, which is a matrix that can be displayed as an image, the first row of pixels represents the number of counts at a single angle. The first row typically represents the angle made from vertical LORs as shown with solid lines in Figure
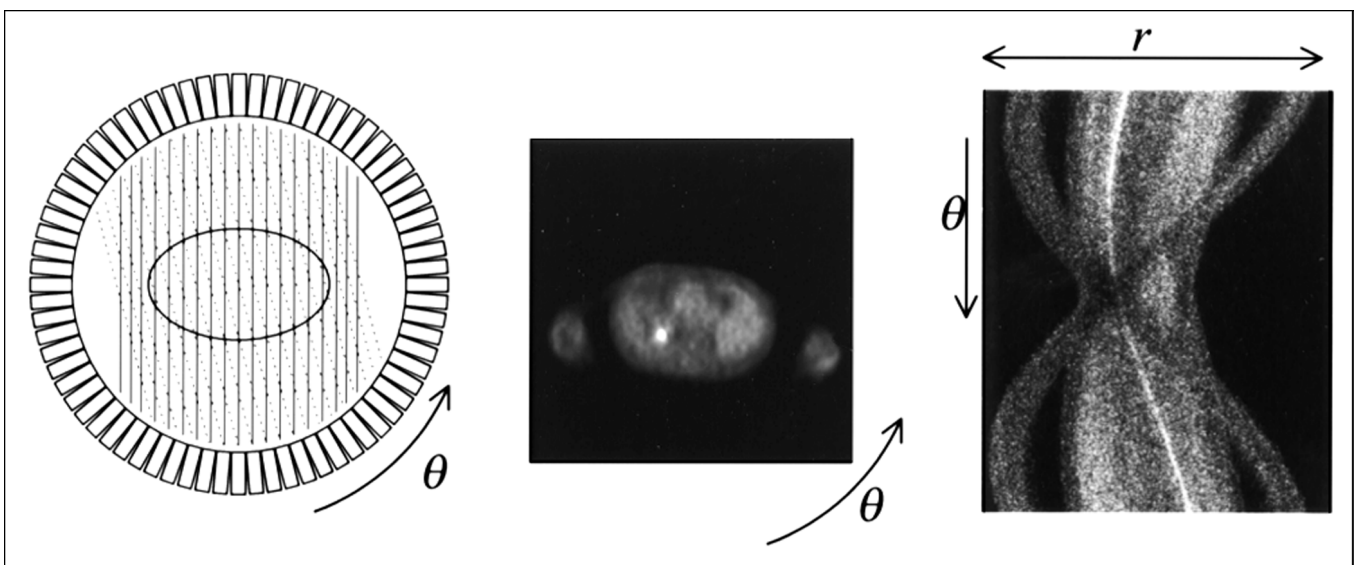

FIGURE 3. At left are detector pairs forming 2 projections, indicated by solid and dashed lines. In the middle is a cross-sectional radioactivity distribution from a patient. At right is the corresponding sinogram. The most notable features in the sinogram are the hot lesion, which is slightly off-center, and the arms, which are at a large radius when viewed at the first and last angles, but cross near the middle when viewed from the middle (horizontal) angles.

3. The next row represents the next angle, which is only slightly different. The row halfway down the sinogram represents the horizontal LORs, and the last row represents the lines almost 180° from the starting lines. Unlike SPECT imaging, in which the LORs are different if measured with the camera below the patient than with the camera 180° around at the top of the patient (because of collimator distance-dependence, attenuation, and scatter effects), all the information in a PET scan can be represented by a 180° angular range.

Image Reconstruction

The raw PET data can be reconstructed into cross-sectional images with the same algorithms as SPECT and x-ray CT. Although it is beyond the scope of this article to discuss reconstruction algorithms, it is important to note the recent addition of iterative algorithms to the capabilities of most commercial systems.

DEGRADING FACTORS

The quality of images produced by a PET system is degraded by several physical factors. Some can be corrected.

Scatter

Consider the in-plane scatter event depicted on the left-hand side of Figure 4. Here, one photon from an annihilation leaves the body unscattered, and the other scatters once before leaving the body. Based on the location of the hit detectors, it appears that the source of the radiation was outside the body. This phenomenon is not possible in single-photon imaging, where the scattered radiation always appears to come from the scattering body. Not all scattered events will scatter in such a way that the source appears to be outside the body.

The degree to which scattered events are accepted depends on the energy resolution of detectors and the associated lower energy threshold of the energy window.

Another scatter possibility is shown on the right-hand side of Figure 4. In this case, the positron emission is outside the plane of the detector ring. One of the annihilation photons is directed toward the ring, and the other one, initially directed further away from the detectors, is scattered back. In this case, radiation outside the detector ring appears to be in the plane of the detectors.
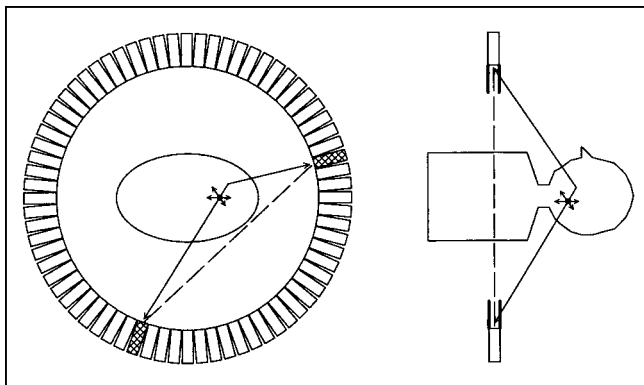

FIGURE 4. Scattered events. At left is in-plane scatter and at right is out-of-plane scatter, rejected by septa.
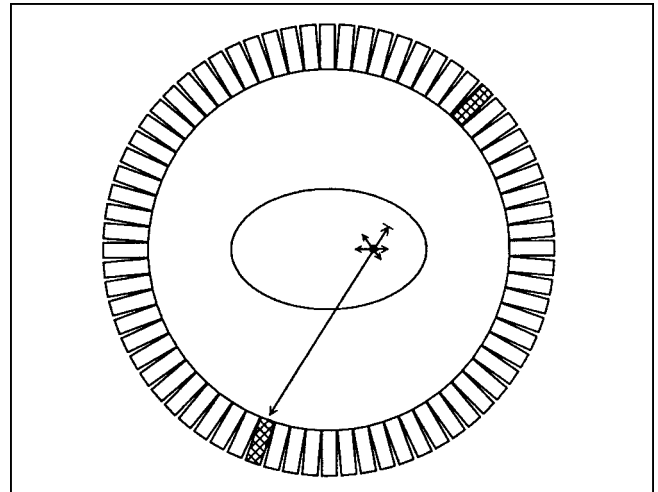

FIGURE 5. Attenuation. One of the photons is stopped or deflected before being detected.

The solution for most out-of-plane scatter is to use shields that block radiation originating outside the field of view (FOV) of the ring. Flat, ring-shaped lead or tungsten septa are used, not only to reduce the number of scattered events collected, but to minimize other effects of radiation originating outside the FOV, including dead-time and random events, discussed later. The effect of septa is to reduce the scatter from 30%–60% of all collected events to approximately 10%–20%. As with single-photon imaging, the number of scattered events collected depends on the size of the body region being imaged and scanner properties. A commonly implemented scatter correction algorithm is described in (1).

Attenuation

Attenuation is the loss of true events due to scatter and absorption. Figure 5 shows an event in which photons were directed toward detectors, but one detector is not hit because the photon is somehow stopped or deflected. This scattered photon may or may not be detected in another detector.

PET attenuation effects differ substantially from single-photon imaging attenuation effects. In PET, both annihilation photons must leave the body unattenuated for the event to be detected. Therefore, the probability that an event will be attenuated is much higher in PET than in single-photon imaging. This is true even though the PET photon energy is much higher than the typical single-photon energy.

One of the unique characteristics of attenuation in coincidence imaging is that, in most cases, at least one of the emitted photons must traverse a substantial amount of tissue, even if the radiation is near the edge of the body.

The most obvious effect of attenuation is overall loss of counts. The result is increased noise and inaccurate quantitation of radioactivity distributions. Although the noise effects cannot be remedied, quantitative accuracy can be recovered with attenuation correction.

Another effect of attenuation is to introduce nonuniformities into reconstructed images. For example, radiation emitted from the middle of the body is more likely to be attenuated than

radiation emitted near the edge. The resulting images will, therefore, show artificially depleted radioactivity deeper in the body. The outer contour of the body shows an artificially high amount of radioactivity because the radiation emitted tangentially to the outer body contour is not attenuated. Because all other radiation emitted from within the body is attenuated in all directions and has no easy path out, a bright outer body contour is observed. If there are concavities in the outer body contour, such as between the legs, the artificially bright contour does not actually dip in, but remains convex.

Less obvious is an effect observed in the lungs. Radiation emitted from within the lungs is less likely to be attenuated than radiation emitted from other nearby regions. The resulting images will therefore show artificially high levels of radioactivity in the lungs.

In some cases, the radiation emitted in selected directions is much more attenuated than radiation emitted in other directions. This is often the case for the bladder, where the lateral diameter is greater than the anterior-posterior (AP), and for lesions near the edge of the body. In these cases, the object will appear elongated along the direction of least attenuation, and depleted regions will result along the other direction. The nature and severity of this problem depend on the particular reconstruction algorithm used.

Figure 6 demonstrates several of the artifacts typical of attenuation.

Attenuation Correction

Two general approaches are used to correct attenuation: calculated correction and measured correction.

A calculated attenuation correction assumes that the outer body contour can be known and that, within this contour, the attenuation properties are constant (e.g., no lungs, no gas, no substantial bone). The outer contour can be determined automatically from the data, or defined by an operator by using an image without attenuation correction.

A measured attenuation correction is done by performing an additional scan. This transmission scan typically uses a radioactive source and the same detectors used for emission
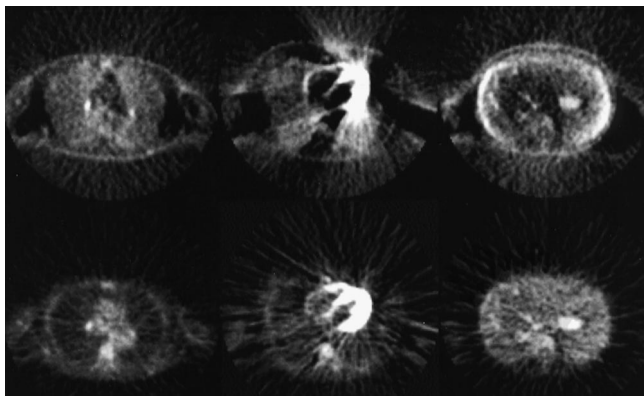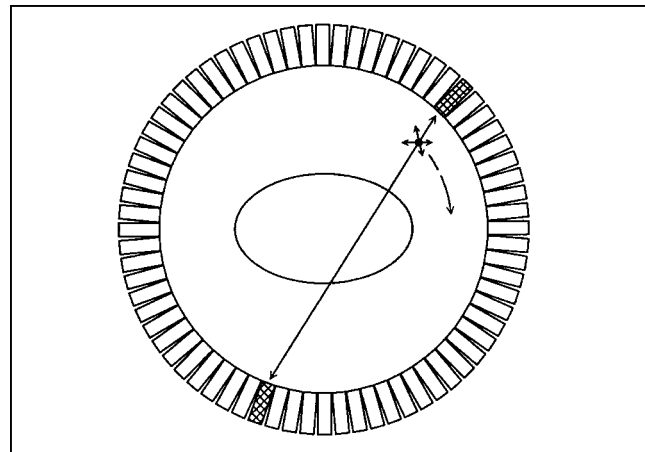

FIGURE 7. Rotating source for transmission scan.

scanning to measure the attenuation of the body along all the LORs, as shown in Figure 7. A reference scan (called the "blank") is performed before any patient transmission scans, and the ratio of the blank counts to the transmission counts during a patient scan yields a correction factor for each emission LOR. The blank scan also serves as a quality assurance measure for the scanner on a daily basis.

Random Events

Even if 2 radiation detectors receive gamma rays at exactly the same time, there will be a difference in the time at which the electronic pulses leave the detectors. The coincidence definition must therefore allow for some difference in detection times. For example, when 1 detector is hit, the system may define a coincidence as any other detector being hit within 6 ns of that detector. The symbol τ is used to represent the total time window, which, in this case (± 6 ns), is 12 ns. This time window must be large enough that all true annihilation events are included. The larger it is, however, the more random events will be recorded. Random events are those in which the 2 photons are not from the same annihilation. The rate of random events between 2 detectors is

$$R_R = \tau \cdot R_1 \cdot R_2, \qquad (3)$$

where R_1 and R_2 are the rates at which detectors 1 and 2 are being hit, and τ is the time window. Random counts add background to the image. Random events become significant (compared with true events) when detector rates are very high, and are more problematic for detectors with low detection efficiency, such as thin sodium iodide, and for three-dimensional imaging.

Dead Time

As the rate of photons hitting a detector increases, the probability of missing a photon due to detector dead time increases. This problem is particularly troublesome for coincidence detection, because both photons must be detected. Dead-time losses are minimized by systems with many independent detectors. Losses are also reduced by faster scintillators and processing electronics.

FIGURE 6. Attenuation effects. At top are images without attenuation correction; at bottom are the same slices with attenuation correction. Noticeable artifacts in the noncorrected images include a bright exterior rim, bright lungs, nonuniform liver, and streaks from the heart.
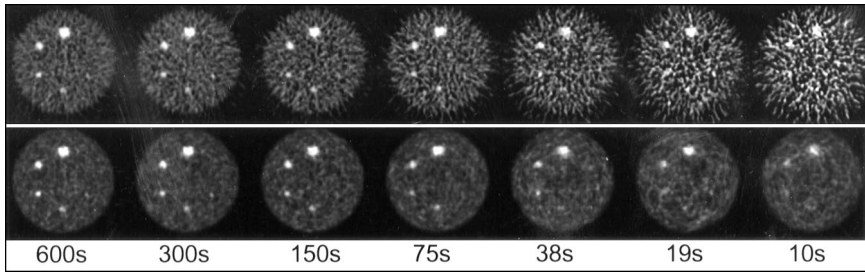
FIGURE 8. Image quality as a function of counts. The same phantom is imaged for various times, increasing approximately at a factor of 2. At top are images reconstructed with filtered back-projection. At bottom are images reconstructed with the ordered subsets algorithm (*2*).

Noise

An important factor in all nuclear medicine images is noise. Image noise (random variations in pixel intensity) is decreased with more counts. More counts are obtained by scanning longer, injecting more radiotracer, or improving the efficiency of the scanner for detecting emitted radiation. In some cases, the amount of tracer cannot be increased because of dead time and random event rate limits in the camera. Figure 8 illustrates the effect of increased counts in hot lesion detection with a single phantom scanned at a range of scan durations.

An important factor in the noise quality of data is the level of background. The counts measured along a particular LOR during a PET scan include true events, random events, and scattered events:

$$P = T + S + R. \quad (4)$$

The true events are obtained by applying scatter and random corrections to the prompt events:

$$T = P - S - R. \quad (5)$$

The total counts measured during the scan is P. The number of counts remaining after correction for scattered random events is T. The number of true events T (after corrections) is not an adequate indicator of subsequent image quality. For example, a study that collected 1 million total counts without any background (no scatter and no random events) would yield much better images than a study with 1.5 million counts, where 0.5 million of the counts are background, even after the background is corrected. In fact, the quality of the images will be similar to those obtained from a 0.7 million-count acquisition with no background. The effect of background on image noise quality is calculated with the noise equivalent count (NEC) formula (*3*). The NEC index allows some comparison to be made between different scanners, or between 2 different operating modes of the same scanner. It is important to note that the index relates only to image noise. A system that is favorable based on NEC considerations may have other disadvantages, such as poor spatial resolution. In addition, a system may not necessarily yield its best images when operating at rates corresponding to its maximum NEC, since spatial and energy resolution can degrade due to pile-up events.

Spatial Resolution

Spatial resolution is an important factor in PET image quality. Several factors impact the spatial resolution obtainable from a scanner:

1. Positron path. The positron travels some distance from the decay to the point where it annihilates, based on its initial energy.
2. Noncollinearity. The annihilation photons are not emitted exactly 180° apart.
3. Detector. In the multidetector PET system discussed thus far, the size of the detector is related directly to spatial resolution. Generally, the smaller the detectors are, the better the spatial resolution. The depth-of-interaction issue puts a limit on resolution, regardless of detector size. A photon trajectory is shown in Figure 9. Such a trajectory could be detected in 1 of several detectors. Conversely, a detector hit by a photon at this angle provides worse localization information than a detector hit head-on. The primary issue is the radial length (thickness) of the detectors. The detector length is usually chosen to give good detection efficiency for 511-keV photons, but in most cases a detector thick enough to stop all 511-keV photons will demonstrate substantial depth-of-interaction uncertainty. A solution is to measure the depth-of-interaction of the photon in the detector, pinpointing the scintillation. This procedure could be done either by using multiple layers of detectors, or by measuring the light on the front and back of the detector and using the difference to indicate the scintillation depth.

HIGH-PERFORMANCE PET SYSTEMS

Current high-performance PET scanners have several common features (*4,5*). One important feature is that there
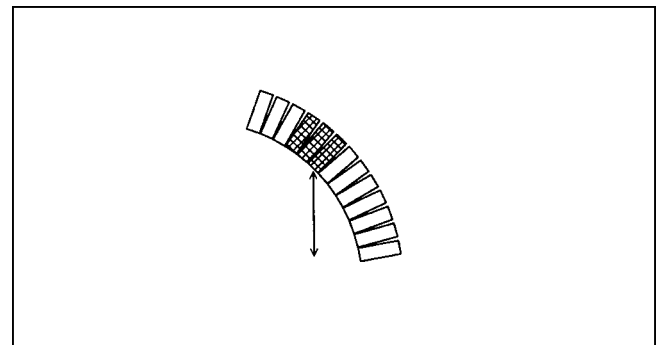

FIGURE 9. Depth-of-interaction problem. Radiation entering the ring from a large radius could be detected in 1 of several detectors, resulting in degraded spatial resolution.
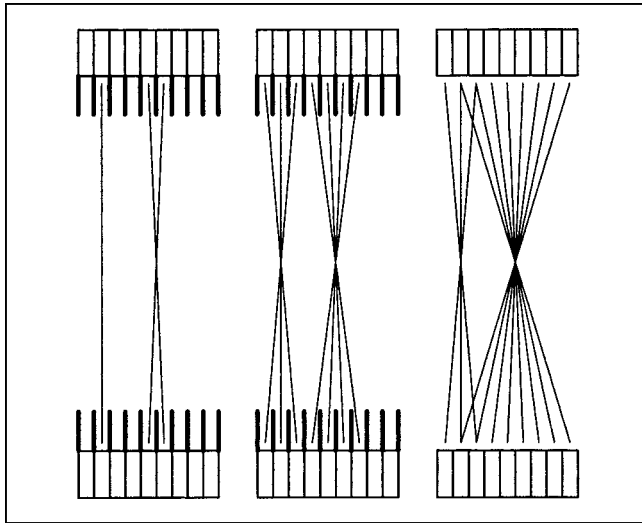
FIGURE 10. Multiring PET acquisition modes. At left are examples of simple 2D direct and cross planes. In the middle are extended 2D direct and cross planes for increased efficiency. At right is full 3D acceptance. The acceptance is greater for radiation in the middle of the axial FOV than for radiation near the end.

TABLE 2
Characteristics of Two High-end Dedicated PET Scanners

Model	GE Advance (4)	CTIECAT EXACT HR + (5)
Block size	6 × 6	8 × 8
Crystal size	4.0 × 8.1 × 30 mm³	4.4 × 4.1 × 30 mm³
No. of rings	18	32
Detectors/ring	672	576
Axial FOV	15.2 cm	15.5 cm
ring diameter	92.7 cm	82.7 cm

are multiple rings of detectors, which extend the axial FOV while maintaining axial resolution.

Figure 10 shows a side view of a multiring tomograph. Image planes are formed from events in which both photons are detected in 1 ring (called "direct planes") and events in which photons are detected in adjacent rings (called "cross planes"). If a system has n rings, then the number of resulting image planes is 2n-1. On current systems with very small detectors, extending the axial acceptance of each plane increases detection efficiency. For example, a direct plane may include events in which the photons were detected in the rings on each side, as shown in the middle of Figure 10.

A large increase in detection efficiency can be obtained by collecting all coincidence events in any detectors, regardless of which rings the detectors are in. For events at large angles to be detected, the septa must be removed. Therefore, scattered coincidence events are a large component of three-dimensional PET data, and more sophisticated scatter correction algorithms must be used (6). An additional problem is that without septa, the detectors are more sensitive to radiation originating outside the scanner's FOV, which in turn increases detector dead time and random events.

With thousands of scintillation detector elements in current PET systems, it is not feasible for each to be coupled to its own photomultiplier. Therefore, an approach is used similar to that used in Anger cameras. Detector crystals are grouped together in blocks, typically 6 × 6 or 8 × 8. Each block is coupled to 4 photomultiplier tubes (PMTs). The total light detected in the tubes is used as a measure of the
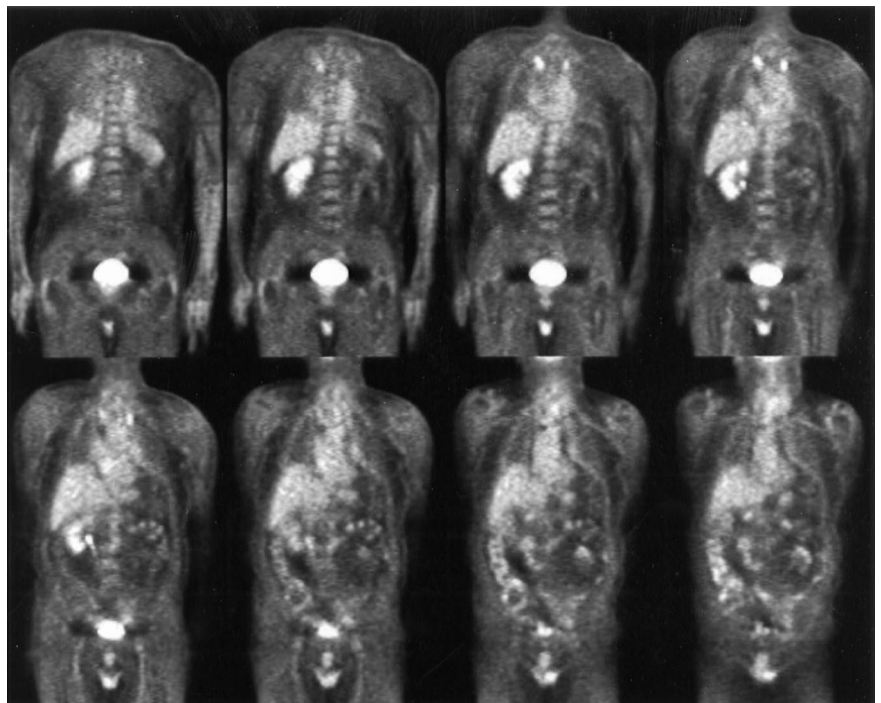

FIGURE 11. A whole-body F-18 fluorodeoxyglucose study from a dedicated PET scanner operating. Total scan time was 42 min.
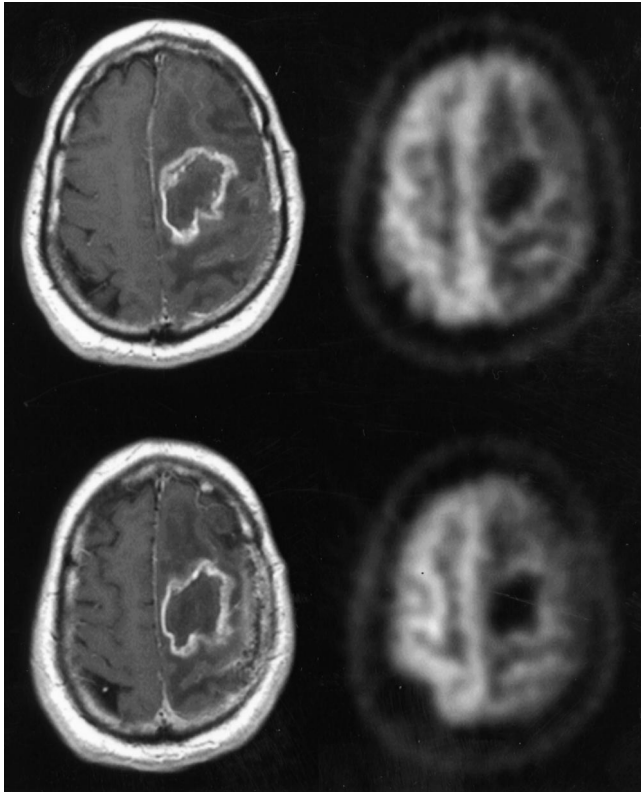
FIGURE 12. An F-18 fluorodeoxyglucose brain tumor study from a dedicated PET scanner operating in 3D mode. Total scan time was 6 min.

incident gamma ray's energy, and the relative light in the tubes is used to determine which crystal was hit. In some cases, the small crystals are separate elements, and in others, the entire block is a single crystal, which is cut into a grid at entrance surface. The positioning logic is not perfect and some events are mislocated, leading to poorer spatial resolution than would be obtained with individually instrumented crystals. However, the benefits (including cost) of using 1 PMT per 9 or 16 detector elements outweigh the problems. Some of the characteristics of 2 available scanners are shown in Table 2.
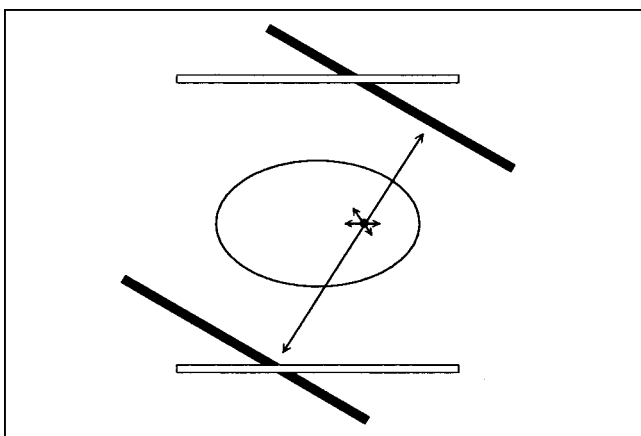

FIGURE 13. Dual-head, rotating gamma camera operating in coincidence mode.

Bismuth germanate (BGO) is the conventional detector material of choice for dedicated PET, because of its high stopping power for 511-keV radiation.

Figures 11 and 12 show typical whole-body and brain studies, respectively, from a multicrystal PET scanner.

HYBRID SYSTEMS

Rotating 2-head gamma cameras provide an alternate means of PET imaging (7). Such systems perform all single-photon-imaging tasks, but are modified to allow coincidence detection, as illustrated in Figure 13. Gamma cameras that have been optimized to image technetium and other low-energy single-photon radionuclides are inherently limited in the quality of PET images that can be produced, as will be discussed. Any modifications made to these systems to optimize their PET performances have 2 realistic constraints: The performance at low energies cannot be compromised substantially, and the cost cannot be raised too much.

The terminology associated with PET imaging on rotating gamma cameras has become very confusing. All tomographic imaging of positron emitters is fairly termed "PET". Also, all positron imaging based on coincidence counting techniques is fairly termed "coincidence" imaging. "PET" and "coincidence" are therefore valid terms for both dedicated PET scanning instruments and for gamma cameras operating in this mode. "PET/SPECT" is a common term, but should be used only to describe a scanner with both capabilities, not a particular way of PET imaging. The term "hybrid" has been officially accepted to describe rotating gamma cameras with PET capability (perhaps prematurely, since it is also a good description of combined nuclear medicine/x-ray CT scanners.)

The specific modifications required to perform PET imaging on a gamma camera are:

Coincidence triggering. Event triggers are generated only when both cameras are hit simultaneously (or within some time window).
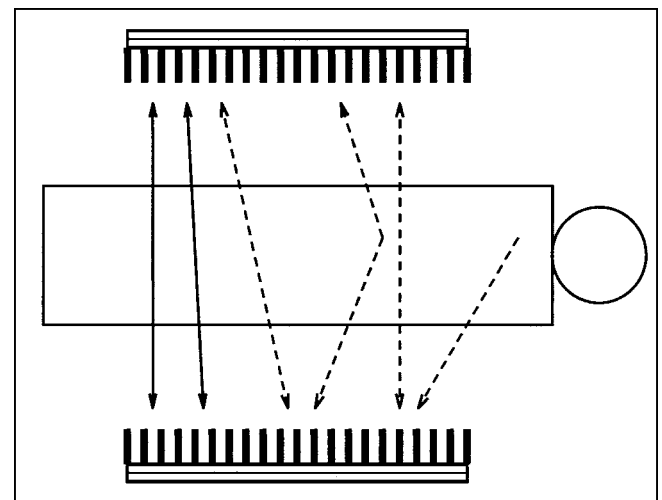

FIGURE 14. The use of septa for hybrid PET imaging. Solid lines represent detected events. Dashed lines represent different types of undetected events.
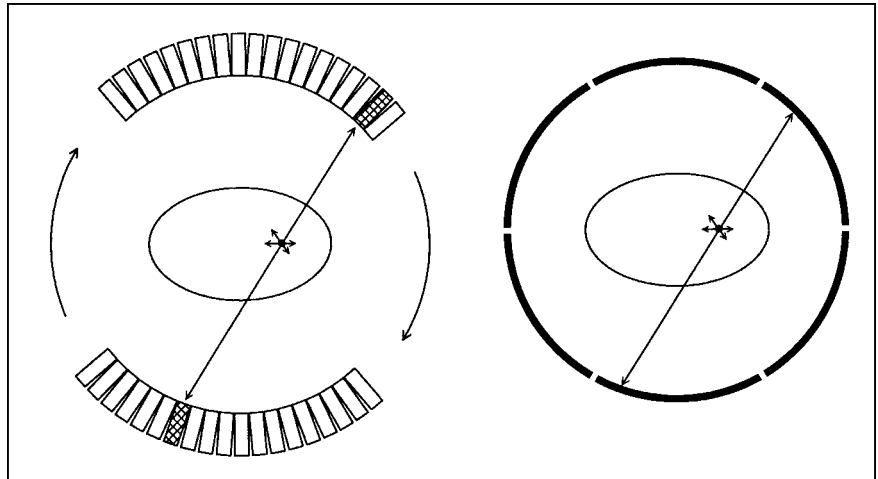
FIGURE 15. Two types of lower-cost dedicated PET scanners.

High-rate capability. The single-photon rates obtained with minimal radioactivity in front of a collimator-less gamma camera are much higher than conventional cameras can handle. Counting rates are improved by various means to facilitate PET imaging.

Crystal thickness. Although it is not a basic requirement, much better images can be obtained with detectors thicker than the standard ⅜-in. Thicknesses of ½-in, ⅝-in, ¾-in, and 1-in have all been implemented.

Collimation. Collimators (multihole or pinhole) are not used for PET imaging. Alternate, less restrictive devices consisting of slats are used, as shown in Figure 14. In principle, no collimation at all is needed. However, rejection of the radiation originating outside the FOV is very helpful on these systems, in addition to the rejection of some scattered events, and the more two-dimensional nature of the data allows simpler reconstruction algorithms.

Whereas the singles counting rates (the rates at which the heads are collecting and processing individual photons) are very high (approximately 1 million counts per s), coincidence counting rates are low. In fact, when a photon is measured in a camera, there is less than a 1% chance of its partner being measured in the opposing camera. This is because of the low detection efficiency, as well as scatter and other effects.

OTHER SYSTEMS

There are 2 types of systems whose performance and price falls between the multicrystal ring systems and rotating gamma camera systems: dedicated NaI PET, and rotating, partial-ring, multicrystal PET, as depicted in Figure 15.

Dedicated NaI PET systems, which have been under development for some time (8), consist of multiple gamma cameras put together to form a full ring. Because these systems are not meant to image the lower energy radiation from single-photon emitters, there are fewer constraints on the crystal thickness than with hybrid systems. The higher energy resolution of NaI (compared with BGO) allows better three-dimensional imaging (due to better rejection of scatter), which helps to compensate for the lower detection efficiency of NaI for 511-keV photons. The systems are still count-rate limited, compared with multicrystal systems, as there are still only 6 gamma cameras, and any scintillation in a camera deadens the vicinity for a substantial time.

Rotating, partial-ring, multicrystal scanners (9) have lower costs associated with them than full-ring multicrystal because of the reduced amount of scintillators and number of photomultipliers. Coincidence detection efficiency is reduced because of the regions of missing detectors, although high singles counting rates are realizable.

REFERENCES

1. Bergstrom M, Eriksson L, Bohmm C, Blomqvist G, Litton J. Correction for scattered radiation in a ring detector positron camera by integral transformation of the projections. *J Comput Assist Tomog*r. 1983;7:42–50.
2. Hudson HM, Larkin RS. Accelerated image reconstruction using ordered subsets of projection data. *IEEE Trans Med Imaging*. 1994;13:601–609.
3. Strother SC, Casey ME, Hoffman EJ. Measuring PET scanner sensitivity: relating countrates to image signal-to-noise ratio using noise equivalent counts. *IEEE Trans Nucl Sci*. 1990;3:783–788.
4. DeGrado TR, Turkington TG, Williams JJ, Stearns CW, Hoffman JM, Coleman RE. Performance characteristics of a whole-body PET scanner. *J Nucl Med*. 1994; 35:1398–1406.
5. Brix G, Zaers J, Adam L-E, et al. Performance evaluation of a whole-body PET scanner using the NEMA protocol. *J Nucl Med*. 1997;38:1614–1623.
6. Ollinger JM. Model-based scatter correction for fully 3D PET. *Phys Med Biol*. 1996;41:153–76.
7. Patton JA, Turkington TG. Coincidence imaging with a dual-head scintillation camera. *J Nucl Med*. 1999;40:432–441.
8. Karp JS, Muehllehner G, Mankoff DA, et al. Continuous-slice PENN-PET: a positron tomograph with volume imaging capability. *J Nucl Med*. 1990; 31:617–27.
9. Townsend DW, Wensveen M, Byars LG, et al. A rotating PET scanner using BGO block detectors: design, performance and applications. *J Nucl Med*. 1993;34:1367–76.